International Conference on Space Optics—ICSO 2008

Toulouse, France

14–17 October 2008

Edited by Josiane Costeraste, Errico Armandillo, and Nikos Karafolas

Multi-parameter fibre Bragg grating sensor-array for thermal vacuum cycling test

L. Cheng

B. Ahlers

P. Toet

G. Casarosa

et al.

International Conference on Space Optics — ICSO 2008, edited by Josiane Costeraste, Errico Armandillo, Nikos Karafolas, Proc. of SPIE Vol. 10566, 105661E · © 2008 ESA and CNES
CCC code: 0277-786X/17/$18 · doi: 10.1117/12.2308294

MULTI-PARAMETER FIBRE BRAGG GRATING SENSOR-ARRAY FOR THERMAL VACUUM CYCLING TEST

L. Cheng(1), B. Ahlers(2), P. Toet(1), G. Casarosa(3), M. Appolloni(3).

(1)TNO Science and Industry, Optics, Stieltjesweg 1, 2600 AD Delft, The Netherlands, lun.cheng@tno.nl.
(2)TNO Science and Industry, Space and Science, Stieltjesweg 1, 2600 AD Delft, The Netherlands, berit.ahlers@tno.nl
(3)AOES Netherlands B.V., Huygensstraat 34, 2201 DK Noordwijk, The Netherlands, gianluca.casarosa@esa.int.

ABSTRACT

Fibre Bragg Grating (FBG) sensor systems based on optical fibres are gaining interest in space applications. Studies on *Structural Health Monitoring* (SHM) of the reusable launchers using FBG sensors have been carried out in the *Future European Space Transportation Investigations Programme* (FESTIP). Increasing investment in the development on FBG sensor applications is foreseen for the *Future Launchers Preparatory Programme* (FLPP). TNO has performed different SHM measurements with FBGs including on the VEGA interstage [1, 2] in 2006.

Within the current project, a multi-parameter FBG sensor array demonstrator system for temperature and strain measurements is designed, fabricated and tested under ambient as well as *Thermal Vacuum* (TV) conditions in a TV chamber of the *European Space Agency* (ESA), ESTEC site. The aim is the development of a multi-parameters measuring system based on FBG technology for space applications. During the TV tests of a *Space Craft* (S/C) or its subsystems, thermal measurements, as well as strain measurements are needed by the engineers in order to verify their prediction and to validate their models. Because of the dimensions of the test specimen and the accuracy requested to the measurement, a large number of observation/measuring points are needed. Conventional sensor systems require a complex routing of the cables connecting the sensors to their acquisition unit. This will add extra weight to the construction under test. FBG sensors are potentially light-weight and can easily be multiplexed in an array configuration.
The different tasks comply of a demonstrator system design; its component selection, procurement, manufacturing and finally its assembly. The temperature FBG sensor is calibrated in a dedicated laboratory setup down to liquid nitrogen (LN_2) temperature at TNO. A temperature-wavelength calibration curve is generated. After a test programme definition a setup in thermal vacuum is realised at ESA premises including a mechanical strain transducer to generate strain via a dedicated feed through in the chamber. Thermocouples are used to log the temperature for comparison to the temperature FBG sensor. Extreme temperature ranges from -150ºC and +70ºC at a pressure down to 10^{-4} Pa (10^{-6} mbar) are covered as well as testing under ambient conditions. In total five thermal cycles during a week test are performed.
The FBG temperature sensor test results performed in the ESA/ESTEC TV chamber reveal high reproducibility (within 1 ºC) within the test temperature range without any evidence of hysteresis. Differences are detected to the previous calibration curve. Investigation is performed to find the cause of the discrepancy. Differences between the test set-ups are identified. Equipment of the TNO test is checked and excluded to be the cause. Additional experiments are performed. The discrepancy is most likely caused by a 'thermal shock' due to rapid cooling down to LN_2 temperature, which results in a wavelength shift.
Test data of the FBG strain sensor is analysed. The read-out of the FBG strain sensor varies with the temperature during the test. This can be caused by temperature induced changes in the mechanical setup (fastening of the mechanical parts) or impact of temperature to the mechanical strain transfer to the FBG.
Improvements are identified and recommendations given for future activities.

1 INTRODUCTION

The development and fabrication of the multi-parameter FBG sensor array is described in Section 2 including the demonstrator system design, its components selection, manufacturing/assembling the sensors and the calibration of the FBG temperature sensor.
Definition of the test programme, system setup in ESA TV chamber, measurements in TV conditions and the test analysis are discussed in section 3 and 4. Finally, conclusions are drawn in Section 5.

2 SENSOR SYSTEM DEVELOPMENT AND FABRICATION

The multi-parameter FBG sensor system as illustrated in Fig. 1 for the demonstration of TV application consists of a broadband light source (BLS), an optical splitter (OS), wavelength detection system (DS), a lead fibre optical cable to connect the light source and the sensors

in the TV chamber, vacuum feed through (FT) for the optical fibre and the multi-parameter FBG sensor array with one FBG temperature sensor (Temp_S) and one strain sensor (Str_S).

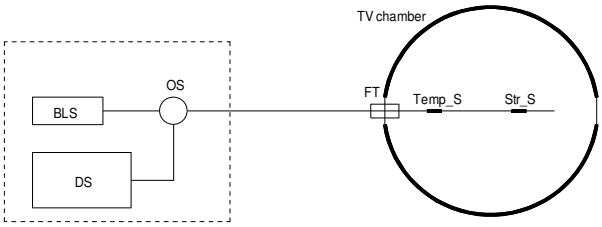

Fig. 1. Setup diagram with broadband light source (BLS), detection system (DS), optical splitter (OS), a vacuum feed through (FT) and the temperature and strain sensor in the thermal vacuum chamber.

2.1 Sensor design

The FBG sensor array consists of a temperature sensor, a strain sensor and optional an existing TNO acceleration sensor. The material in the latter is found to be not fully vacuum compatible and is skipped in the test programme.

To ensure easy handling of the sensors, both the temperature sensor and the strain sensor are mounted to an aluminium housing. The designs are shown in Fig. 2.

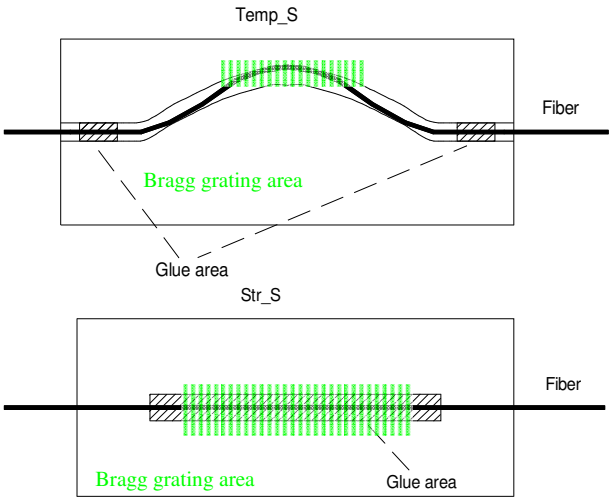

Fig. 2. Sketch of temperature sensor (top) and the strain sensor (bottom).

The FBG strain sensor will be tested by mounting it to a plate. Bending the plate will generate surface strain which can be measured by the FBG strain sensor.

2.2 Strain transducer for the TV chamber

To generate a strain signal to the FBG strain sensor which is mounted on a bending plate, a mechanical strain transducer is designed. The strain can be varied via an existing mechanical feed-through available in the TV chamber. Using an off-axis mounted cylinder (Fig. 3a), a rotation of the feed-through will be converted to a centre displacement variation of the bending plate (Fig. 3b) on which the FBG strain sensor is attached. The turning wheel of the feed-through is shown in Fig 4.

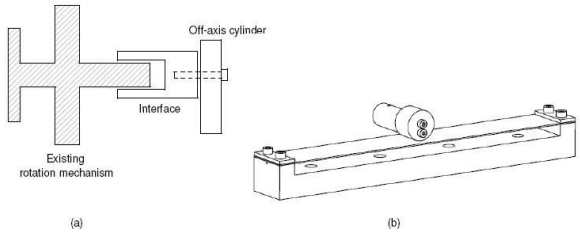

Fig. 3. Sketch of test setup using existing rotation mechanism (a) to generate surface strain in a bending plate via an off-axis mounted cylinder (b). The FBG is mounted beneath the bending plate.

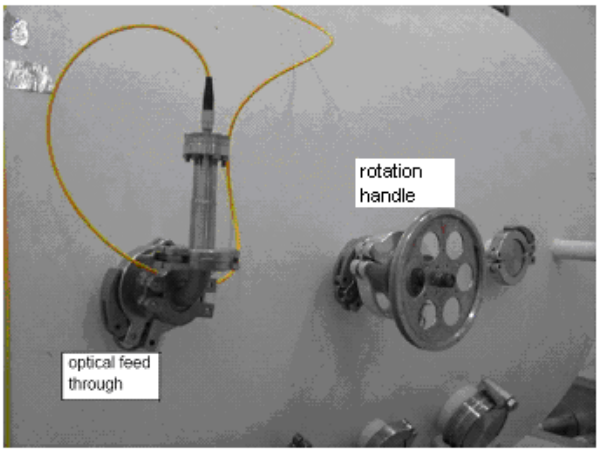

Fig 4. The turning wheel at the outer side of the TV chamber.

2.3 Detection system

Two detection systems for FBG sensors are available at TNO: the commercial system MicronOptics si425 and the TNO demonstrator DEMINSYS [3]. The latter is developed for high speed measurements up to about 20 kHz. Since no high speed event is expected within the test when the FBG acceleration sensor is skipped, and the si425 is regarded to be a mature system with proper data logging mode, the si425 is selected as the detection system for the FBG sensor array.

2.4 Coating for optical fibre and FBG

Standard acrylate coating for optical fibre cannot be used in TV chamber due to outgassing. Polyimide coating for the optical fibre and FBG is selected. The FBGs are recoated with polyimide.

2.5 Optical feed through for TV chamber

A vacuum feed through for a single-mode (SM) fibre at 1550 nm, with a core diameter of about 9 µm and

cladding diameter of 125 µm is selected and used for the test in the TV chamber.

2.6 Adhesive

An adhesive conform the European Cooperation for Space Standardization (ECSS) have to be selected and used to glue the fibre. The Stycast 2850FT is selected. After procurement and manufacturing of the components/parts, an FBG temperature sensor and an FBG strain sensor in an array configuration are realised.

3 TESTS

3.1 Test of temperature sensor

After the integration, the response of the FBG temperature sensor is measured at TNO. A Pt100 is attached to the FBG temperature sensor for reference purposes. The test is performed down to LN_2 temperature by immersing the FBG temperature sensor in a LN_2 bath (Fig 5). The temperature of the FBG sensor reaches the LN_2 temperature within tens of seconds. After vaporising of the LN_2, the temperature of the sensor increases gradually to room temperature. The duration of the warming up process is about 3 hours.

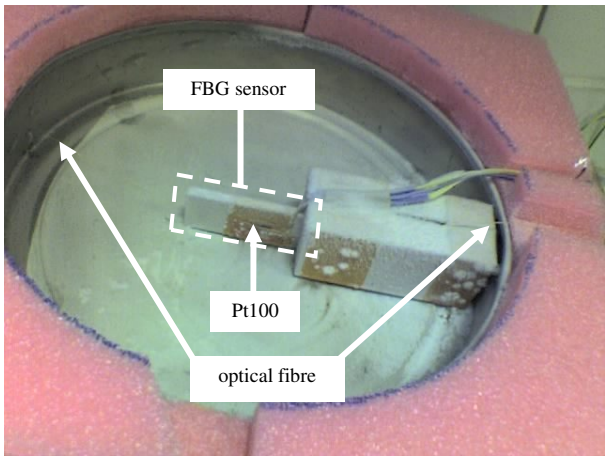

Fig. 5. Test setup at TNO to test the FBG temperature sensor down to LN_2 temperature.

The temperature measured by the Pt100 and the wavelength of the FBG temperature sensor are used to generate a temperature-wavelength curve. Only the slow warming up part of the measurement can be used. Three tests are performed. The three curves match well (see Fig 6). The maximum deviation is at the lowest temperature (<0.03nm at LN_2 temperature). This can be caused by an error in the timing between the FBG temperature sensor system and that of the Pt100.

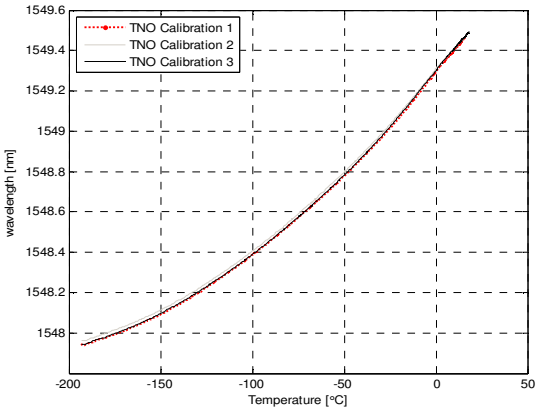

Fig. 6. Results of the 3 temperature measurements at TNO.

3.2 Test campaign under TV conditions

A test programme is developed for testing the FBG temperature sensor and the FBG strain sensor at both the ambient conditions (temperature / pressure) and at a pressure down to 10^{-4} Pa (10^{-6} mbar) during temperature cycling.

A TV chamber made available by ESA/ESTEC is used to test the FBG sensor array under TV conditions (see Fig. 7).

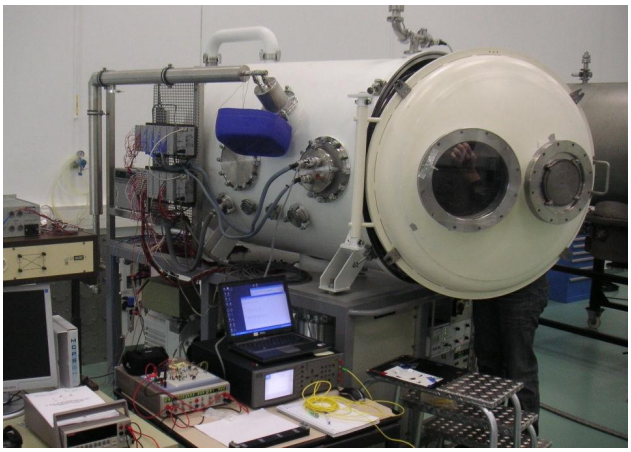

Fig. 7. The TV chamber made available by ESA used in this test programme.

The temperature in the TV chamber can be varied. The TV chamber is equipped with a number of conventional electrical temperature sensors. The FBG temperature sensor can be tested by comparing the response with the measured temperature. In Fig. 8 a photo of the FBG sensor array installed in the TV chamber is shown. The installation of the FBG sensor array in the TV chamber is carried out by ESA.

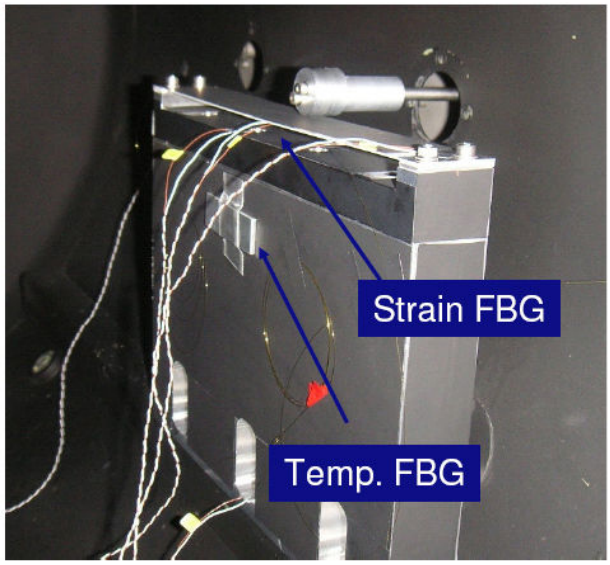

Fig. 8. Location of the FBG sensors. Strain sensor on the bending plate and temperature sensor on an aluminium block.

The temperature cycles measured by one of the conventional electrical temperature sensor (thermo couple) is presented in Fig. 9. The cycling is divided into two Data Logging (DL) sections: DL2 and DL3. DL2 covers the first two cycles until t is about 2 times 10^5s.

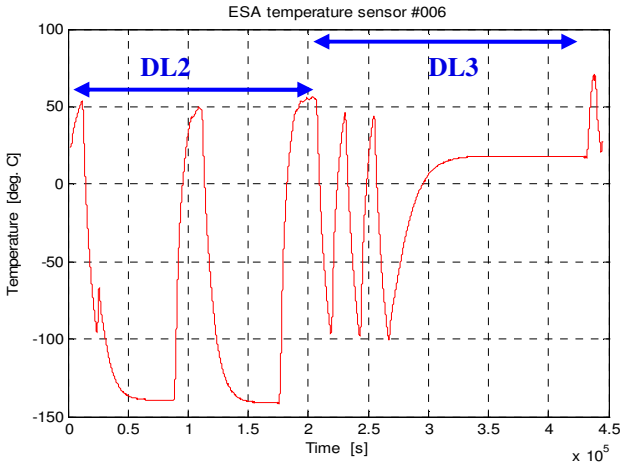

Fig. 9. Temperature measured by electrical temperature sensor #006 during DL2 and DL3. Bake out (70 ˚C) is performed at the end of the temperature cycling.

The following tests are designed and performed during the test campaign:

FBG temperature sensor test:
- Data Logging (DL) of the readout of the FBG during different pressure changes and temperature cycles for comparison with conventional temperature sensor.

FBG strain sensor test using bending plate setup:
- Strain Measurements (SM) at different temperatures during the temperature cycling (Fig. 9) are carried out by several turns of the turning wheel as described in section 2.2. Rotation direction will be alternated between *Counter-ClockWise* (CCW) and C*lockWise* (CW). The rotation will cause a centre displacement of the bending plate varying between 0.5mm and 3.5mm. The wavelength shift corresponds to the amplitude of the strain variation is measured and compared.

4 TEST RESULTS

During the TV test, the wavelength of the FBG sensors and the temperature measured by the thermocouples are logged. The data for the different tests are analysed.

4.1 FBG temperature sensor

The temperature measurement is performed during temperature cycling (DL2 and DL3). The temperature development during DL2 and the corresponding wavelength of the FBG temperature sensor are presented in Fig. 10.

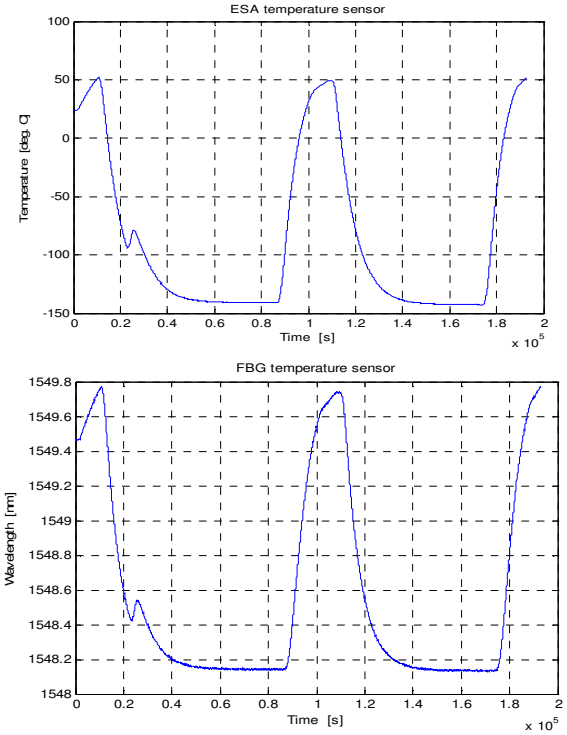

Fig. 10. Temperature measured by conventional sensor (top). Wavelength shift of the FBG temperature sensor at the same location (bottom).

To verify if there are any hysteresis in the FBG temperature sensor, the data during cooling down (2x) and warming up (2x) in DL2 are processed separately. The deviation is found to be less than 0.01nm. No hysteresis is observed.

The data of DL3 including the bake out and about 30 h constant temperature is processed. The temperature-wavelength curve for DL2 and DL3 presented in the figure below. The results of DL2 and DL3 show a great reproducibility. The difference is less than 0.01nm. The temperature coefficient at 20˚C is found to be 0.01 nm/K, which is equal to the typical value presented in literature for FBG based on standard single mode fibre operating near 1550 nm [4]. This coefficient depends on the composition of the fibre. The temperature coefficient decreases with lower temperature. For -100˚C, the coefficient is 0.007 nm/K.

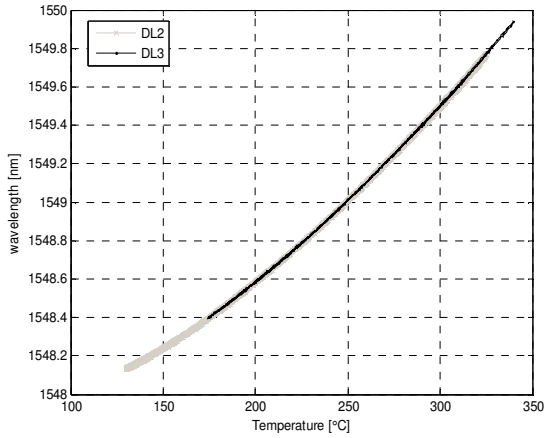

Fig. 11. Temperature-wavelength curve calculated from DL2/3. This includes 5 temperature cycles and a bake out over 5 days.

Comparing this result with the test result of the TNO test in LN_2 bath as discussed in section 3.1, reveals a discrepancy for temperature higher than -50˚C. The difference is about 0.1 nm at 20˚C.

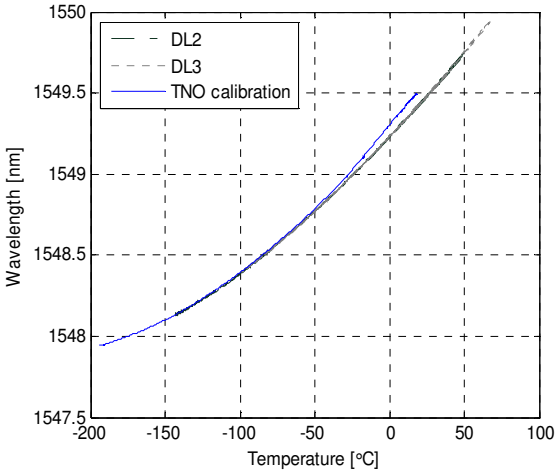

Fig. 12. Comparison between the test results at TNO (calibration 3) and at ESA (DL2 and DL3).

In order to understand this discrepancy, the LN2-bath test at TNO has been repeated. An extra wavelength increase of about 0.07 nm following by a relaxation effect after a few hours has been spotted. The wavelength increase and the relaxation are found to be caused by the thermal shock on the FBG by immersing it in the LN_2 bath. These phenomena, as far as know, have not been reported before. The results of the extra LN_2 test at TNO after the TV tests match very well with the previous TNO tests. The maximum deviation is about 0.01 nm. This demonstrates the high reproducibility of the FBG temperature sensor.

4.2 Strain Measurements

A number of *Strain Measurement* (SM) is performed within the temperature cycling during DL2 and DL3. Each SM includes minimum four turns (CCW-CW-CCW-CW) of the turning wheel (Fig. 13). The wavelength shift for the CCW rotations is lower than for CW rotations. The difference is about 10%. The possible reason seems to be the friction.

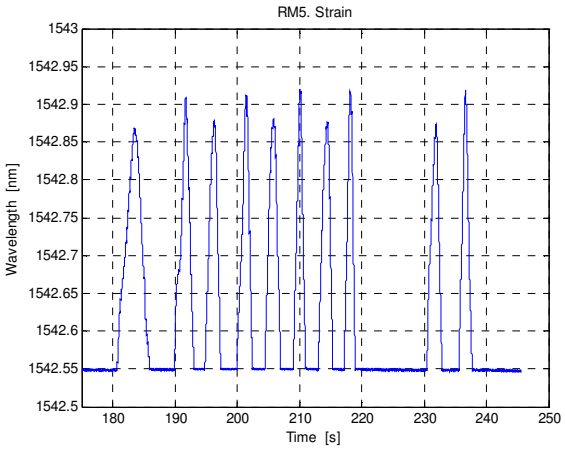

Fig. 13. FBG strain sensor response during a Strain Measurement.

The SM's are performed during the temperature cycling. The effect of the SM's can be observed as extra wavelength change on top of the thermal expansion of the bending plate which is also measured by the FBG strain sensor (Fig. 14 top).

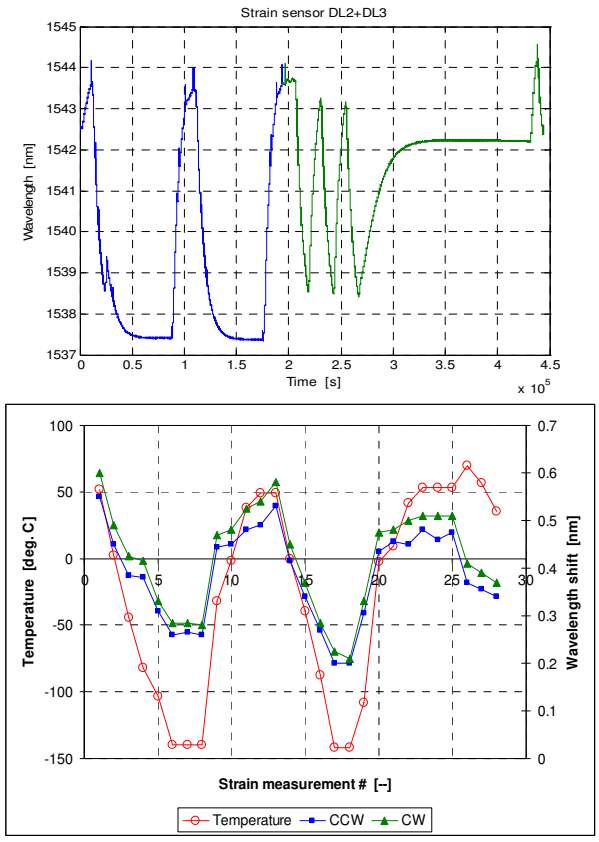

Fig. 14. FBG strain sensor readout of the SM (top). The amplitude of the wavelength shift peak during CCW and CW rotations are summarised (bottom).

The wavelength shift of the SM's, as presented in Fig. 13 is measured and compared (Fig. 14 bottom). The wavelength shift decreases with the temperature. This is probably caused by the change of the fastening of the bolts in the mechanical setup for transferring the rotation of the turning wheel to a displacement of the bending plate (see Fig. 3). A slow degeneration of the wavelength shift in Fig. 14 is also observed. This can be explained by the influence of temperature to the glue and/or the polyimide coating of the FBG.

5 CONCLUSION AND OUTLOOK

A Multi-parameter FBG sensor array for temperature and strain sensing is designed and realized using components suitable for TV applications (polyimide coated fiber/FBG and successfully tested under TV conditions).

Tests of the temperature sensor at TNO demonstrate the sensor can be used down to LN_2 temperature. Good reproducibility is shown. The response of the FBG temperature sensor in the TV test reproduces very well for the test range from -150 ºC to +70 ºC. No noticeable hysteresis is observed between cooling down and heating up during 5 thermal cycles in 5 days. The deviation is found to be less than 0.01nm. A discrepancy is found between the results of the TNO pre-tests in LN2 and the TV tests. Additional test at TNO is carried out and we noticed an extra wavelength increase (about 0.07nm) of the FBG temperature sensor after a thermal shock due to rapid cooling down to LN_2 temperature. This effect disappears after some time. This effect can be eliminated by using non-coated FBG.

In the Strain Measurements, the wavelength shift of the FBG strain sensor decreases with the temperature. This can be caused by a variation in the fastening of the bolt that fixes the rotating arm to the mechanical feed through. Furthermore, a degeneration effect of the FBG strain sensor can be observed. This effect is more obvious during and after bake out at about 70 ˚C. This problem can be caused by the glue and/or the polyimide coating of the FBG. Suitable glue for the strain sensor to ensure constant strain transfer to the FBG has to be investigated.

6 ACKNOWLEDMENT

This work has been realised under the combined efforts of TNO and the ESA under the networking and partnering programme; ESTEC contract number 20317/07/NL/EM.

7 REFERENCES

1. Cheng L.K., B. Ahlers, *International Conference on Space Optics (ICSO), ESA SP-621*, ESTEC, Noordwijk, 2006.

2. Cheng L.K., B. Ahlers, *International Conference on Optical Fibre Sensors (OFS-18)*, Mexico, 2006.

3. Cheng L.K., J.J.M. Groote Schaarsberg and B.W. Oostdijk, *First European Workshop on Structural Health Monitoring*, July 2002.

4. Hirayama N. and Y. Sano, *ISA Transactions 39*, 169-173, 2000.